ARTICLES

Pyruvate kinase M2 is a phosphotyrosine-binding protein

Heather R. Christofk[1], Matthew G. Vander Heiden[1,3], Ning Wu[1], John M. Asara[2,4] & Lewis C. Cantley[1,4]

Growth factors stimulate cells to take up excess nutrients and to use them for anabolic processes. The biochemical mechanism by which this is accomplished is not fully understood but it is initiated by phosphorylation of signalling proteins on tyrosine residues. Using a novel proteomic screen for phosphotyrosine-binding proteins, we have made the observation that an enzyme involved in glycolysis, the human M2 (fetal) isoform of pyruvate kinase (PKM2), binds directly and selectively to tyrosine-phosphorylated peptides. We show that binding of phosphotyrosine peptides to PKM2 results in release of the allosteric activator fructose-1,6-bisphosphate, leading to inhibition of PKM2 enzymatic activity. We also provide evidence that this regulation of PKM2 by phosphotyrosine signalling diverts glucose metabolites from energy production to anabolic processes when cells are stimulated by certain growth factors. Collectively, our results indicate that expression of this phosphotyrosine-binding form of pyruvate kinase is critical for rapid growth in cancer cells.

Metabolic regulation in rapidly growing tissues such as fetal tissues and tumours is different from that in most adult tissues. Rapidly growing cells must take up nutrients at a high rate and maintain a balance between utilization of nutrients for energy production (for example, ATP synthesis) and for anabolic processes (for example, protein, lipid and nucleic acid synthesis). In contrast, most adult tissues require less nutrient uptake and use a greater fraction of available nutrients for energy production rather than macromolecule synthesis. This difference between metabolism of cancer cells and normal adult tissues was first pointed out by Warburg in 1929[1], who observed that cancer cells take up glucose at higher rates than normal tissue but use a smaller fraction of this glucose for oxidative phosphorylation, even when oxygen is not limiting. This effect, called aerobic glycolysis or the Warburg effect, is thought to be due to the reprogramming of metabolic genes to allow cancer cells to function more like fetal cells and to enable a greater fraction of glucose metabolites to be incorporated into macromolecule synthesis rather than burned to CO_2.

More recent studies have shown that growth factor signalling pathways have a major role in programming metabolic pathways in cells by mediating long-term[2,3] as well as acute[4] changes in cell metabolism. Paradoxically, there are reports that activation of protein-tyrosine kinases results in a decrease in the specific activity of pyruvate kinase, the enzyme that catalyses the penultimate step in glycolysis; that is, conversion of phosphoenolpyruvate to pyruvate[5,6]. The mechanism by which protein-tyrosine kinases affect the activity of pyruvate kinase has been controversial. Pyruvate kinase as well as several other enzymes involved in glycolysis (including enolase and lactate dehydrogenase) are phosphorylated on tyrosine residues in cancer cells[7,8], and it has been argued that the inhibition of pyruvate kinase observed in cells with activated protein-tyrosine kinases could be explained by direct tyrosine phosphorylation[9,10]. However, others have argued that the stoichiometry of tyrosine phosphorylation of pyruvate kinase (and of other glycolytic enzymes) is too low to affect catalytic activity. Here we present a novel mechanism to explain how protein-tyrosine kinases acutely regulate the activity of pyruvate kinase.

Screen identifies PKM2 as a pTyr binding protein

We used a proteomic screening approach to identify novel phosphotyrosine (pTyr)-binding proteins from cell lysates (Fig. 1a). Using SILAC, stable isotope labelling of amino acids in cell culture[11], we prepared lysates from HeLa cells grown in either heavy isotopic ^{13}C-arginine and ^{13}C-lysine or normal isotopic ^{12}C-arginine and ^{12}C-lysine. 'Heavy' lysates were flowed over a phosphotyrosine peptide library affinity matrix, and 'light' lysates were flowed over a corresponding unphosphorylated peptide library affinity matrix. Bound proteins were eluted with sodium phenylphosphate, digested with trypsin, and the peptides were analysed by microcapillary liquid chromatography tandem mass spectrometry (LC-MS/MS). As shown in Fig. 1b, most of the proteins identified had peptides that yielded ~1:1 SILAC heavy to light ratios, thus indicating equal binding to the phosphotyrosine and tyrosine peptide matrices. As a validation of the approach, several proteins that contain well-characterized phosphotyrosine-binding domains were identified as showing >3:1 SILAC ratios, consistent with preferential binding to the phosphotyrosine peptide library affinity matrix. Surprisingly, despite the absence of a known phosphotyrosine-binding domain, pyruvate kinase exhibited a ≥15:1 SILAC heavy:light ratio, identifying it as a candidate novel phosphotyrosine-binding protein.

As validation of the phosphotyrosine-binding property of pyruvate kinase, lysates from HeLa cells were passed over the phosphotyrosine and tyrosine peptide library affinity matrices, and eluates were analysed by SDS–polyacrylamide gel electrophoresis (PAGE). LC-MS/MS analysis of those proteins visible by silver stain that selectively bound to the phosphotyrosine peptide library matrix also identified known phosphotyrosine-binding proteins as well as pyruvate kinase (Fig. 1c). To confirm the preferential binding of pyruvate kinase to the phosphotyrosine peptide affinity matrix, eluates from the phosphotyrosine and tyrosine peptide library columns were analysed by western blot using a pyruvate kinase antibody (Fig. 1d). p85, the SH2-domain-containing regulatory subunit of phosphatidylinositol-3 kinase, is used as a positive control, and GAPDH is used as a negative control. As shown in Fig. 1d, immunoblotting for both p85 and pyruvate kinase shows selective binding to the phosphotyrosine

[1]Department of Systems Biology, [2]Department of Pathology, Harvard Medical School, Boston, Massachusetts 02115, USA. [3]Dana Farber Cancer Institute, Boston, Massachusetts 02115, USA. [4]Division of Signal Transduction, Beth Israel Deaconess Medical Center, Boston, Massachusetts 02115, USA.

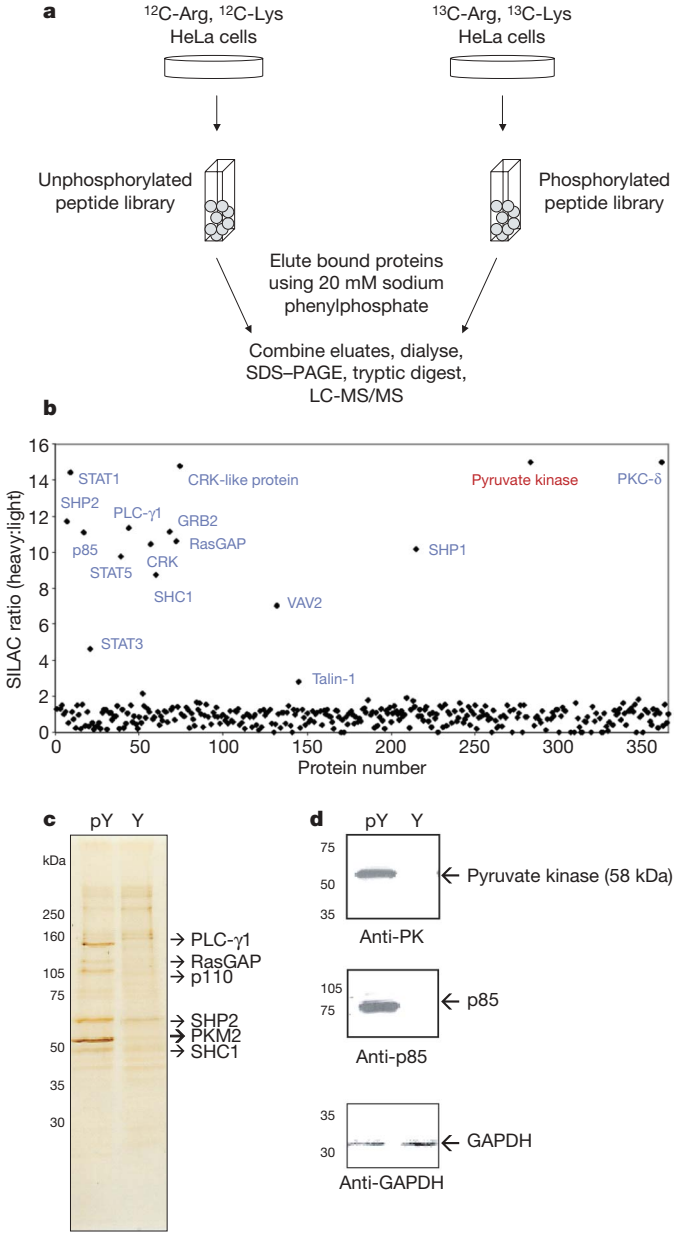

Figure 1 | Proteomic screen identifies pyruvate kinase as a novel phosphotyrosine-binding protein. **a**, A schematic diagram of the proteomic screen for phosphotyrosine binding proteins using SILAC and peptide library affinity matrices. The peptide libraries were designed as follows: phosphorylated peptide library (pY), biotin-Z-Z-Gly-Gly-Gly-X-X-X-X-X-pTyr-X-X-X-X-X-Gly-Gly; unphosphorylated peptide library (Y), biotin-Z-Z-Gly-Gly-Gly-X-X-X-X-X-Tyr-X-X-X-X-X-Gly-Gly, where Z indicates aminohexanoic acid and X denotes any amino acid except cysteine. Peptide libraries were incubated with streptavidin beads and packed onto columns to form the phosphotyrosine and tyrosine peptide library affinity matrices. Heavy lysates were flowed over the phosphotyrosine column, and light lysates were flowed over the tyrosine column. Bound proteins were eluted with 20 mM sodium phenylphosphate, digested with trypsin, and then analysed by microcapillary reversed-phase tandem mass spectrometry (LC-MS/MS). **b**, Screen results using commercially available software showing the SILAC ratios (heavy:light) for the proteins identified by LC-MS/MS. Background proteins yielded ~1:1 SILAC ratios. Known phosphotyrosine-binding proteins (blue) yielded >3:1 SILAC ratios. Pyruvate kinase (red) yielded a ≥15:1 SILAC ratio, identifying it as a candidate novel phosphotyrosine binder. **c**, A silver stain of proteins from HeLa cell lysates that bound to the phosphotyrosine compared with tyrosine peptide library columns. Differentially stained proteins identified by LC-MS/MS are indicated. **d**, Immunoblotting of proteins from HeLa cell lysates that bound to the phosphotyrosine versus tyrosine peptide library columns. Eluates from the columns were immunoblotted with antibodies for pyruvate kinase, p85 as a positive control, and GAPDH as a negative control.

peptide library matrix. Notably, whereas pyruvate kinase exhibited selective binding to the immobilized phosphotyrosine peptide library, it did not show selective binding to immobilized phosphoserine or phosphothreonine peptide libraries (Supplementary Fig. 1).

pTyr binding is specific to pyruvate kinase isoform M2

Four pyruvate kinase isoforms exist in mammals: L, liver; R, red blood cell; M1, adult; and M2, embryonic/tumour[12] (Fig. 2a). The M1, M2 and L isoforms were transiently expressed as Flag-tagged proteins in 293 cells, and lysates were flowed over the phosphotyrosine and tyrosine peptide affinity columns to assess binding. Eluates from the columns were analysed by western blot using a Flag antibody (Fig. 2b). The M2 isoform is the only pyruvate kinase isoform that binds phosphotyrosine peptides. Given that PKM1, the splice variant of PKM2, does not bind to phosphotyrosine peptides, we looked to the crystal structures of these isoforms for a potential phosphotyrosine-binding site on PKM2. PKM1 and PKM2 are identical proteins with the exception of a 56-amino-acid stretch encoded by the alternatively spliced region. Previous studies have shown that this stretch of amino acids comprises the only structural difference between the M1 and M2 isoforms and forms an allosteric pocket unique to PKM2 that allows for binding of its activator, FBP[13].

To determine whether the FBP-binding pocket on PKM2 coordinates phosphotyrosine peptide binding, we assessed whether FBP could compete for binding of PKM2 to a phosphotyrosine peptide library column. Recombinant PKM2 was incubated with increasing amounts of FBP and then flowed over the phosphotyrosine peptide affinity matrix. A concentration of 20 μM FBP was able to compete for binding of recombinant PKM2 to phosphotyrosine peptides (Fig. 2c). To examine further how this region of PKM2 interacts with phosphotyrosine, point mutants of various residues in and around

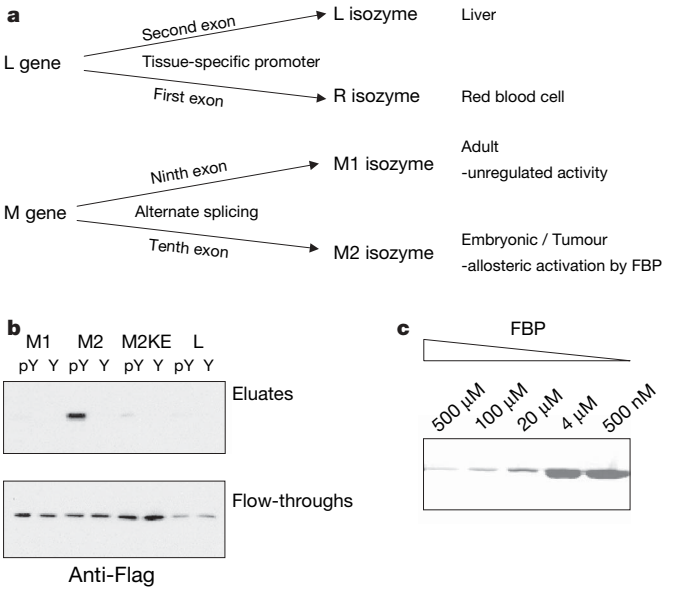

Figure 2 | Phosphopeptide binding is specific to the M2 isoform of pyruvate kinase and involves lysine 433 near the FBP binding pocket. **a**, A schematic diagram of the four mammalian pyruvate kinase isoforms. **b**, Immunoblotting showing the pyruvate kinase isoform specificity of phosphotyrosine binding. The M1, M2, M2KE and L Flag-tagged pyruvate kinase isoforms were transiently expressed in 293 cells, and lysates were flowed over the phosphotyrosine (pY) and tyrosine peptide library columns. The flow-throughs and eluates from the columns were immunoblotted with Flag antibody. Note that M2KE stands for the K433E point mutant of PKM2. **c**, A Coomassie stain of PKM2 bound to the phosphotyrosine peptide library column after incubation with increasing amounts of FBP. Recombinant PKM2 was incubated with increasing concentrations of FBP as indicated, before being flowed over and eluted from the phosphotyrosine peptide library affinity matrix with sodium phenylphosphate.

the FBP-binding pocket of PKM2 were constructed. Whereas mutation of residues within the FBP-binding pocket of PKM2 did not affect phosphotyrosine peptide binding (data not shown), mutation of lysine 433—located within the unique region of PKM2, which lies at the lip of the pocket—to glutamate abolished phosphotyrosine peptide binding (Fig. 2b). Note that the K433E (KE) point mutant of PKM2 that lacks phosphotyrosine peptide binding ability still gets activated by FBP to a similar degree as the wild-type protein (Supplementary Fig. 2). These data suggest that phosphotyrosine peptides are binding to PKM2 near the FBP-binding pocket of the enzyme and that lysine 433 is important for this interaction.

To examine the allosteric FBP-binding pocket of PKM2 more closely, we used X-ray crystallography to re-solve the structures of both the *apo*-form (2.5 Å) as well as the FBP-bound form (2 Å) of PKM2. Both forms crystallized as tetramers in the asymmetric units under physiological pH, with Mg^{2+} and oxalate in the active sites (Supplementary Table 1). In the *apo* crystal, the residues around the FBP-binding pocket are not well ordered. In particular, loop W515–G520 has no visible electron density. In comparison, FBP is found in all four allosteric sites in the complex crystal (Fig. 3a), and its presence stabilizes many residue side chains including the W515–G520 loop, K433 and W482 (Fig. 3b). In the FBP-bound form of PKM2, the W515–G520 loop and other side chains are closed down on the FBP molecule, and only the P1 phosphate group of FBP is solvent accessible (Fig. 3c). These differences between the two structures are not unexpected; however, it was surprising to find FBP bound in any of the crystals as no FBP was added during any stage of protein purification. The fact that ~50% of PKM2 still retained FBP after affinity purification, dialysis and size exclusion column chromatography suggests that the release of FBP from the protein is very slow.

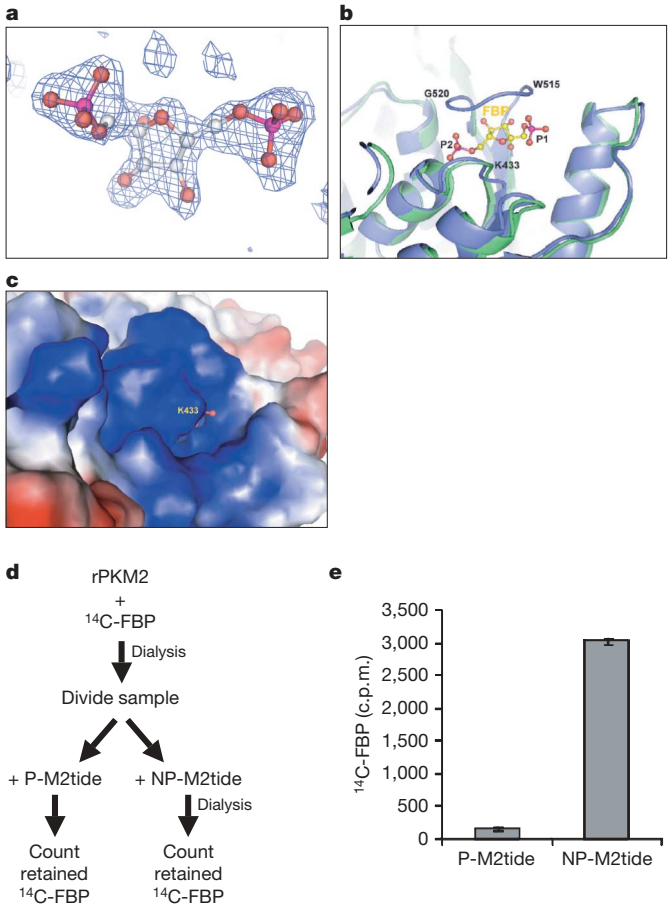

Figure 3 | Phosphotyrosine peptide catalyses the release of FBP from PKM2. **a**, Representative composite omit $2F_o - F_c$ electron density for FBP contoured at the 1.2 σ level. **b**, A close up of the allosteric pocket of PKM2 showing an overlay of the FBP-bound form (blue) and the *apo*-bound form (green). The flexible FBP activation loop including residues W515–G520 is structured in the FBP-bound form of PKM2, but not in the *apo* form of PKM2. **c**, Surface electrostatic potential of the FBP binding pocket in the same orientation as in **b**. The bound FBP is completely enclosed by the protein except for the P1 phosphate group. Basic moieties on the protein surface are shown in blue; acidic moieties are shown in red. **d**, A schematic diagram of the experiment to test the effect of phosphotyrosine peptide binding on FBP release from PKM2. First, recombinant PKM2 was soaked in ^{14}C-FBP, and unbound FBP was removed by dialysis. Then the FBP-loaded PKM2 was incubated with P-M2tide or NP-M2tide, and the unbound FBP was removed by dialysis. ^{14}C-FBP retained on PKM2 was measured using a scintillation counter. **e**, ^{14}C scintillation counts retained on the recombinant PKM2 after exposure to P-M2tide versus NP-M2tide. Error bars denote s.e.m. ($n = 3$).

Published K_d (dissociation constant) values for FBP binding to PKM2 are in the micromolar range[14]; however, FBP concentrations after protein purification would be orders of magnitude lower than this value. Our attempts to measure the dissociation constant based on Michaelis–Menten kinetics have suggested that FBP binding to PKM2 is nonlinear. To test the hypothesis suggested by the above structural studies that FBP binds tightly to PKM2, we soaked recombinant PKM1 and PKM2 in ^{14}C-FBP, removed unbound FBP by dialysis, and measured the ^{14}C-FBP retained on the proteins by scintillation counting. After dialysis overnight, the PKM1 sample had the same amount of ^{14}C-FBP as the no-protein control sample. In contrast, the PKM2 sample exhibited 52 ± 5% more ^{14}C counts than both the PKM1 sample and the no-protein control. On further analysis we have estimated that ^{14}C-FBP is retained at roughly half a mole per mole on the PKM2 protein. Because 50% of the recombinant protein already had bacterial FBP bound, these results are consistent with the retained ^{14}C-FBP being tightly bound to the protein.

pTyr peptide catalyses the release of FBP from PKM2

To examine the effect of phosphotyrosine peptide binding on FBP-bound PKM2, we obtained a peptide binding motif for PKM2 using traditional peptide library screening, and synthesized both the phosphorylated and unphosphorylated versions of the optimal peptide: P-M2tide (GGAVDDDpYAQFANGG) and NP-M2tide (GGAVDDDYAQFANGG), respectively (Supplementary Fig. 3). We then incubated our ^{14}C-FBP-loaded recombinant PKM2 with P-M2tide or NP-M2tide, dialysed away unbound FBP and peptide, and measured the counts retained on PKM2 (Fig. 3d). Exposure of PKM2 to the control NP-M2tide resulted in a significant amount of FBP remaining bound to PKM2. In contrast, exposure of PKM2 to the P-M2tide resulted in release of the majority of the FBP (Fig. 3e). These results indicate that phosphotyrosine peptide binding catalyses the release of FBP from PKM2.

Next we tested whether phosphotyrosine protein binding can catalyse the release of FBP from PKM2 in cells. To address this, we cultured cells overnight with ^{3}H-glucose that can be metabolized to ^{3}H-FBP. We then immunoprecipitated Flag-tagged PKM2, and determined the amount of ^{3}H bound to PKM2 with and without pervanadate treatment by scintillation counting. Increasing the levels of phosphotyrosine proteins by a 15-min treatment with pervanadate resulted in a 30 ± 13% reduction in ^{3}H that immunoprecipitated with PKM2. These results support the hypothesis that phosphotyrosine protein binding can catalyse the release of FBP from PKM2 *in vivo*.

pTyr binding results in inhibition of PKM2 activity

To examine the effect that phosphotyrosine peptide binding has on PKM2 activity, we incubated increasing amounts of P-M2tide and NP-M2tide with recombinant PKM2 and measured the enzyme activity. As shown in Fig. 4a, P-M2tide exposure causes a 20–30% inhibition of PKM2 activity in a dose-dependent manner. Multiple phosphotyrosine peptides comprising *in vivo* phosphorylation sites previously identified on metabolic proteins[15] were synthesized

(Supplementary Table 2). Several of these phosphotyrosine peptides, as well as multiple phosphotyrosine peptides designed after known tyrosine kinase motifs, were also shown to inhibit PKM2 activity (Fig. 4b). Notably, the Src kinase motif, along with the *in vivo* Src kinase sites on enolase and lactate dehydrogenase, were able to inhibit PKM2 activity *in vitro*. Consistent with a catalytic FBP-release mechanism of P-M2tide enzyme inhibition, longer exposures of P-M2tide to recombinant PKM2 consistently result in greater decreases in PKM2 activity (data not shown). In addition, as little as 1 μM phosphotyrosine peptide can inhibit PKM2 activity, suggesting that a meaningful interaction between PKM2 and tyrosine-phosphorylated proteins can occur at the concentrations present in cells (Fig. 4a).

To address further whether PKM2 activity can be regulated by tyrosine phosphorylation levels in cells, we elevated phosphotyrosine levels in various cell lines by pervanadate stimulation, and measured pyruvate kinase activity. As shown in Fig. 4c, pervanadate stimulation in three different cancer cell lines resulted in a 20–30% decrease in total pyruvate kinase activity. To assess whether tyrosine kinase intracellular signalling could regulate PKM2 activity in cells, we tested the effects of overexpressing a tyrosine kinase and stimulating an RTK signalling pathway. Transient overexpression of constitutively active Src kinase in 293 cells resulted in inhibition of PKM2 activity (Fig. 4d). Additionally, acute stimulation of tyrosine kinase signalling by insulin-like growth factor (IGF) stimulation in A549 cells resulted in inhibition of PKM2 activity (Fig. 4e). Consistent with earlier studies from Eigenbrodt and co-workers[5], our data show that conditions that activate protein-tyrosine kinases in cells in culture result in an acute ~15% to 30% reduction in the activity of pyruvate kinase.

Cancer cell lines exclusively express the M2 isoform of pyruvate kinase[5]. However, to confirm that the decrease in pyruvate kinase activity on increasing phosphotyrosine levels was specific to the M2 isoform of pyruvate kinase and that it depended on the ability of PKM2 to bind to phosphotyrosine peptides, we constructed cell lines that express the M1, M2, L, or M2KE (phosphotyrosine-binding mutant) forms of pyruvate kinase (Fig. 4f). We made stable H1299 cells that express Flag-tagged mouse M1, M2, M2KE, or L, and then stably knocked down the endogenous (human) PKM2 using short hairpin (sh)RNA expression. As shown in Fig. 4f, we obtained efficient knockdown of the endogenous PKM2, and the Flag-tagged rescue proteins were expressed to similar, near endogenous, levels. Increased phosphotyrosine levels observed on pervanadate stimulation of the M1-, M2-, M2KE- and L-expressing knockdown cells resulted in specific inhibition of pyruvate kinase activity only in the wild-type M2-expressing cells (Supplementary Fig. 4 and Fig. 4g). Together, these data suggest that the regulation of pyruvate kinase activity by phosphotyrosine levels in cells is specific to the M2 isoform and requires the phosphotyrosine peptide binding capability. Similar results were also obtained in A549 cells (data not shown).

Cell growth requires the pTyr-binding function of PKM2

To determine whether regulation of PKM2 activity by phosphotyrosine peptide binding has a biological role in the cell, we assessed the ability of the phosphotyrosine-binding mutant, M2KE, to rescue M2 knockdown in cancer cell lines. Knockdown of PKM2 expression in H1299 lung cancer cells results in reduced glycolysis and decreased cell proliferation (Fig. 5a, b). Both the wild-type mouse M2 and mouse M2KE rescue pyruvate kinase activity (data not shown) and

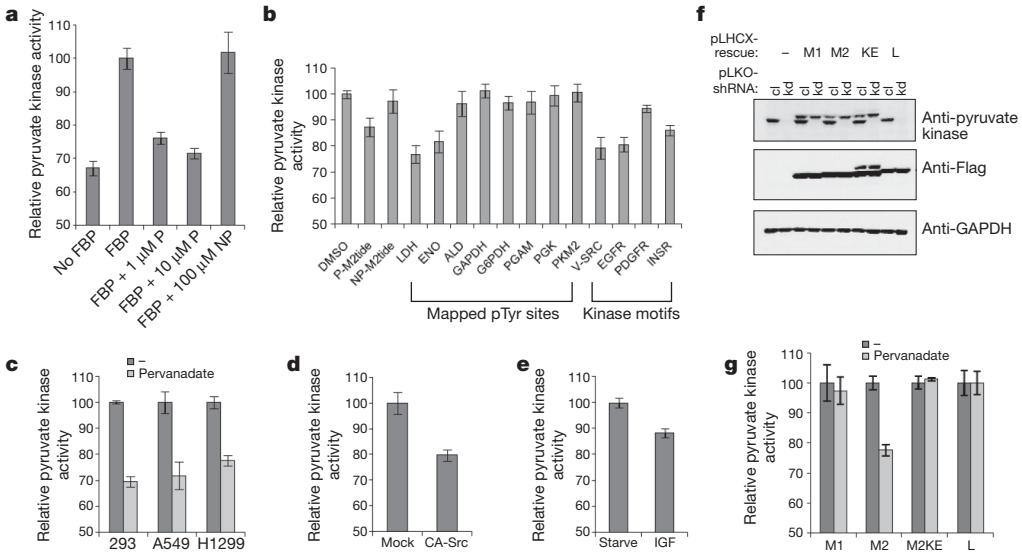

Figure 4 | Phosphopeptide binding results in inhibition of PKM2 activity. **a**, Comparison of pyruvate kinase activity in the presence of FBP, P-M2tide (P) and NP-M2tide (NP). Recombinant PKM2 was soaked in FBP, unbound FBP was removed by dialysis, and then 1 μM P-M2tide, 10 μM P-M2tide, or 100 μM NP-M2tide was added to the enzyme. After a 30-min incubation at room temperature, unbound FBP and peptide were removed by dialysis, and pyruvate kinase activity was assessed. **b**, Comparison of pyruvate kinase activity in the presence of various phosphotyrosine peptides. FBP-soaked recombinant PKM2 was incubated with 10 μM peptide for 10 min at room temperature and pyruvate kinase activity was assessed. Eight of the phosphopeptides tested comprised previously mapped phosphotyrosine sites on the metabolic proteins indicated. Four of the phosphopeptides tested were designed after known tyrosine kinase motifs. Because all of the peptides were dissolved in DMSO, DMSO was used as a negative control. **c**, Comparison of pyruvate kinase activity in lysates from 293, A549 and H1299 cells with and without (−) pervanadate stimulation. **d**, Comparison of pyruvate kinase activity in lysates from 293 cells that were mock-transfected (mock) or transiently transfected with constitutively active Src kinase (CA-Src). **e**, Comparison of pyruvate kinase activity in lysates from A549 cells serum-starved overnight without (starve) or with 15 min of 20 nM IGF stimulation (IGF). **f**, Immunoblotting of lysates from H1299 cells stably expressing shRNA constructs and rescue constructs. Cells were infected with retrovirus containing the empty vector (pLHCX), or pLHCX with Flag-tagged mouse PKM1 (M1), mouse PKM2 (M2), mouse PKM2 KE point mutant (KE), or PKL (L). After 2 weeks selection in hygromycin, the cells were infected with lentivirus containing the pLKO vector with control shRNA (cl) or shRNA that knocks down PKM2 expression (kd). The cells were then selected in puromycin for 1 week. Total cell extracts were immunoblotted with antibodies for pyruvate kinase (recognizes both M1 and M2), Flag and GAPDH. Note that PKL is not recognized by the pyruvate kinase antibody. **g**, Comparison of pyruvate kinase activity in lysates from H1299 cells expressing knockdown shRNA and Flag–PKM1, PKM2, PKM2 KE and PKL with and without pervanadate stimulation. All scale bars denote s.e.m. ($n = 3$). In all cases, the changes in pyruvate kinase activity were significant as assessed by Student's t-test ($P < 0.01$).

glycolysis in PKM2 knockdown cells (Fig. 5a). Flow cytometry analysis indicates similar cell death, cell size and cell cycle profiles in the M2- and M2KE-expressing knockdown cells (data not shown). However, unlike the wild-type mouse M2, the mouse M2KE mutant is unable to rescue the decreased cell proliferation observed in the knockdown cells. These data suggest that the phosphotyrosine-binding ability of PKM2, although dispensable for the role of PKM2 in glycolysis under cell culture conditions, is important for its role in cell proliferation. Similar results were also obtained in A549 cells (data not shown).

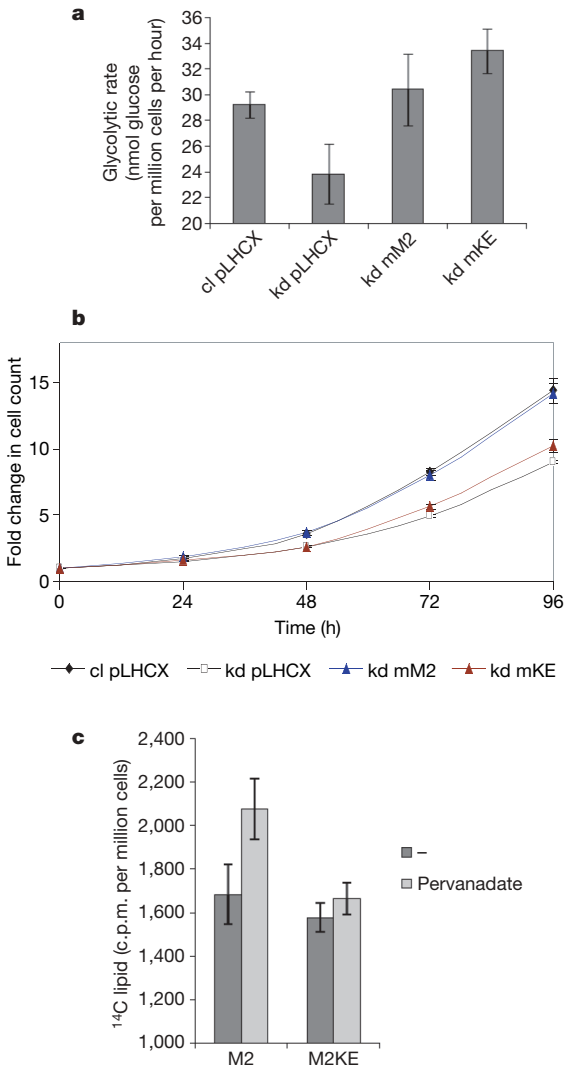

Figure 5 | The phosphopeptide binding ability of PKM2 is important for cell proliferation. cl pLHCX, cells with empty rescue vector and control shRNA; kd pLHCX, cells with empty rescue vector and knockdown shRNA; kd mM2, cells with Flag-tagged mouse PKM2 rescue and knockdown shRNA; kd mKE, cells with Flag-tagged mouse PKM2 KE point mutant rescue and knockdown shRNA. **a**, Glucose metabolism rates of the knockdown and rescue H1299 cells. **b**, Proliferation curves of the knockdown and rescue H1299 cells. Error bars in **a** and **b** denote s.e.m. ($n = 3$). At 96 h, the decreased proliferation of the mKE cells as compared with the mM2 cells was statistically significant, as assessed by Student's *t*-test ($P < 0.01$). **c**, ^{14}C incorporation into lipid in ^{14}C-glucose-pulsed cells treated or untreated (−) with pervanadate. M2 indicates cells expressing Flag-tagged mouse PKM2 and knockdown shRNA, and M2KE indicates cells expressing Flag-tagged mouse PKM2 KE point mutant and knockdown shRNA. Cells were pulsed with 2 μCi ml^{-1} of ^{14}C-glucose for 5 min before treatment with pervanadate for 10 min and then lipid extraction. ^{14}C counts in the lipid fractions were measured by scintillation counting. Error bars denote s.e.m. ($n = 6$). The increased incorporation of ^{14}C into lipid observed in the M2 cells after pervanadate stimulation was statistically significant as assessed by Student's *t*-test ($P < 0.05$).

Inhibition of PKM2 by pTyr affects cellular metabolism

Our recent studies have shown that PKM2 is necessary for aerobic glycolysis in tumour cells[16]. Replacement of PKM2 with its more active splice variant, PKM1, was shown to result in reversal of the Warburg effect as judged by reduced lactate production and increased oxygen consumption. Because disruption of phosphotyrosine binding observed in the M2KE mutant is predicted to result in a more active PKM2 enzyme, we assessed whether the phosphotyrosine-binding ability of PKM2 is important for its role in aerobic glycolysis by measuring lactate production and oxygen consumption in cells expressing the M2KE point mutant. Notably, similarly to the changes that were observed when PKM2 was replaced by PKM1 (ref. 16), we observed a 36 ± 3% reduction in lactate production and 24 ± 4% increase in oxygen consumption in the M2KE-expressing cells when compared with the M2-expressing cells. These results suggest that tyrosine kinase regulation of PKM2 activity is involved in mediating the Warburg effect in tumour cells.

No changes in adenine nucleotide levels or the ATP/ADP ratios were observed in M2- versus M2KE-expressing cells, suggesting that this cannot account for the defect in cell proliferation observed in the M2KE-expressing cells. However, acute inhibition of PKM2 activity in proliferating cells by tyrosine kinase signalling may result in a temporary build-up of upstream glycolytic intermediates that can be used by the cell as precursors for fatty acid and nucleic acid synthesis, which could provide an advantage to PKM2-expressing cells for proliferation. Consistent with this model, we observed a 25% increase in the incorporation of metabolites from ^{14}C-glucose into lipids on pervanadate treatment of PKM2-expressing cells. Notably, no significant increase in ^{14}C incorporation into lipids is seen in pervanadate-treated cells expressing the KE point mutant of PKM2 deficient in phosphotyrosine binding (Fig. 5c). A similar increase in the incorporation of ^{14}C-glucose metabolites into lipids was observed on pervanadate stimulation of 293 cells (data not shown). In addition, acute pervanadate stimulation resulted in a 36 ± 1% decrease in oxygen consumption in PKM2-expressing cells with only a 15 ± 4% decrease in oxygen consumption in M2KE-expressing cells. These results demonstrate that phosphotyrosine-based regulation of PKM2 activity has consequences for metabolism in tumour cells and support the idea that regulation of PKM2 activity by tyrosine kinase signalling may enable glucose metabolites to be used for anabolic processes.

Conclusions

We have shown that the activity of the glycolytic protein PKM2 can be regulated by tyrosine kinase signalling pathways via a novel phosphotyrosine-binding ability. Binding of phosphotyrosine peptides to PKM2 catalyses the release of FBP and subsequent inhibition of enzymatic activity. We propose that phosphotyrosine protein binding is a transient event that results in a conformational change in PKM2 structure that releases an otherwise tightly bound FBP molecule. Once released the ambient concentration of FBP at the time of the collision determines whether PKM2 goes into a low activity state or rebinds FBP and is reactivated. In this model, PKM2 only has the ability to undergo dynamic regulation by FBP (as occurs with bacterial, yeast and liver forms of pyruvate kinase) if a tyrosine kinase pathway is activated. We suspect that this mechanism evolved to ensure that fetal tissues only use glucose for growth when they are activated by appropriate growth factor receptor protein-tyrosine kinases. Cancer cells, by re-expressing PKM2, acquire the ability to use glucose for anabolic processes.

Because proliferating cells require *de novo* fatty acid synthesis as well as DNA replication, one possible model is that regulation of PKM2 activity allows for a balance between ATP production and fatty acid/nucleic acid production. Alternatively, phosphotyrosine-based regulation of PKM2 enzymatic activity may provide a direct link between cell growth signals using tyrosine kinases and control of glycolytic metabolism. Regardless, these data demonstrate a novel

mechanism for phosphotyrosine-based regulation of a metabolic protein that is important for cell proliferation.

METHODS SUMMARY

Biotinylated peptide libraries were incubated with streptavidin beads and placed onto columns to construct peptide library affinity matrices. Five milligrams of SILAC lysates, made from HeLa cells as described[11], were flowed over affinity matrices, and bound proteins were digested with trypsin and analysed by microcapillary LC-MS/MS. SILAC ratios were determined using the Paragon algorithm in ProteinPilot software. Human PKM2 was cloned into pET-28a, expressed in bacteria, and purified as an amino-terminally tagged 6×His fusion protein. PKM2 crystals were grown by the hanging-drop method, and the structure was solved by molecular replacement. The binding motif for PKM2 was determined by flowing a phosphotyrosine-oriented degenerate peptide library over 6×His–PKM2-conjugated nickel beads. Bound peptides were sequenced by Edman degradation. For FBP-release analysis, recombinant pyruvate kinase was incubated with ~10 μM ^{14}C-FBP for 30 min, dialysed for >7 h, then incubated with 1 mM peptide for 30 min, and dialysed again for >7 h before sample recovery and scintillation counting. Pyruvate kinase activity was assessed using a continuous assay coupled to lactate dehydrogenase. For cell line construction, Flag-tagged mouse pyruvate kinase isoforms were cloned into pLHCX and used to make retrovirus to infect H1299 and A549 cells. After 2 weeks of selection in 350 μg ml^{-1} hygromycin, the stable cells expressing Flag-tagged mouse pyruvate kinase were infected with lentivirus containing knockdown or control shRNA towards human *PKM2*. These cells were selected for 1 week in 2 μg ml^{-1} puromycin before experimentation. Cellular glucose metabolism rates were measured by following the conversion of 5-^{3}H-glucose to $^{3}H_2O$ as described previously[4]. Cellular proliferation rates were determined by seeding 5×10^4 cells in triplicate in 6-well plates and taking cell counts every 24 h using a Coulter particle analyser for a 3–5-day period. Oxygen consumption and lactate production were measured as described previously[16]. ^{14}C-containing lipids were measured as described previously[17].

Full Methods and any associated references are available in the online version of the paper at www.nature.com/nature.

Received 8 November 2007; accepted 3 January 2008.

1. Warburg, O. On the origin of cancer cells. *Science* **123,** 309–314 (1956).
2. Lum, J. J. *et al.* The transcription factor HIF-1α plays a critical role in the growth factor-dependent regulation of both aerobic and anaerobic glycolysis. *Genes Dev.* **21,** 1037–1049 (2007).
3. Majumder, P. K. *et al.* mTOR inhibition reverses Akt-dependent prostate intraepithelial neoplasia through regulation of apoptotic and HIF-1-dependent pathways. *Nature Med.* **10,** 594–601 (2004).
4. Vander Heiden, M. G. *et al.* Growth factors can influence cell growth and survival through effects on glucose metabolism. *Mol. Cell. Biol.* **21,** 5899–5912 (2001).
5. Eigenbrodt, E., Reinacher, M., Scheefers-Borchel, U., Scheefers, H. & Friis, R. Double role for pyruvate kinase type M2 in the expansion of phosphometabolite pools found in tumor cells. *Crit. Rev. Oncog.* **3,** 91–115 (1992).
6. Zwerschke, W. *et al.* Modulation of type M2 pyruvate kinase activity by the human papillomavirus type 16 E7 oncoprotein. *Proc. Natl Acad. Sci. USA* **96,** 1291–1296 (1999).
7. Reiss, N., Kanety, H. & Schlessinger, J. Five enzymes of the glycolytic pathway serve as substrates for purified epidermal-growth-factor-receptor kinase. *Biochem. J.* **239,** 691–697 (1986).
8. Sale, E. M., White, M. F. & Kahn, C. R. Phosphorylation of glycolytic and gluconeogenic enzymes by the insulin receptor kinase. *J. Cell. Biochem.* **33,** 15–26 (1987).
9. Presek, P., Reinacher, M. & Eigenbrodt, E. Pyruvate kinase type M2 is phosphorylated at tyrosine residues in cells transformed by Rous sarcoma virus. *FEBS Lett.* **242,** 194–198 (1988).
10. Mazurek, S., Grimm, H., Boschek, C. B., Vaupel, P. & Eigenbrodt, E. Pyruvate kinase type M2: a crossroad in the tumor metabolome. *Br. J. Nutr.* **87** (suppl. 1), S23–S29 (2002).
11. Ong, S. E. & Mann, M. A practical recipe for stable isotope labeling by amino acids in cell culture (SILAC). *Nature Protocols* **1,** 2650–2660 (2006).
12. Jurica, M. S. *et al.* The allosteric regulation of pyruvate kinase by fructose-1,6-bisphosphate. *Structure* **6,** 195–210 (1998).
13. Dombrauckas, J. D., Santarsiero, B. D. & Mesecar, A. D. Structural basis for tumor pyruvate kinase M2 allosteric regulation and catalysis. *Biochemistry* **44,** 9417–9429 (2005).
14. Yamada, K. & Noguchi, T. Nutrient and hormonal regulation of pyruvate kinase gene expression. *Biochem. J.* **337,** 1–11 (1999).
15. Villen, J., Beausoleil, S. A., Gerber, S. A. & Gygi, S. P. Large-scale phosphorylation analysis of mouse liver. *Proc. Natl Acad. Sci. USA* **104,** 1488–1493 (2007).
16. Christofk, H. R. *et al.* The M2 splice isoform of pyruvate kinase is important for cancer metabolism and tumour growth. *Nature* doi:10.1038/nature06734 (this issue).
17. Hatzivassiliou, G. *et al.* ATP citrate lyase inhibition can suppress tumor cell growth. *Cancer Cell* **8,** 311–321 (2005).

Supplementary Information is linked to the online version of the paper at www.nature.com/nature.

Acknowledgements We thank W. Hahn for providing the lentiviral shRNA. We thank M. Liu for technical assistance. We thank J. Lee for help in developing the affinity purification techniques. M.G.V.H. is a Damon Runyon Fellow supported by the Damon Runyon Cancer Research Foundation. This research was supported by funding to L.C.C. from the National Institutes of Health.

Author Information PKM2 structure files are deposited in the Protein Data Bank under accession codes 3BJT (*apo* form) and 3BJF (FBP-bound form). Reprints and permissions information is available at www.nature.com/reprints. Correspondence and requests for materials should be addressed to L.C.C. (lcantley@hms.harvard.edu).

METHODS

Peptide library and column construction. A phosphotyrosine peptide library (pY) and its unphosphorylated counterpart (Y) were constructed as follows: pY, biotin-Z-Z-Gly-Gly-Gly-X-X-X-X-X-pTyr-X-X-X-X-X-Gly-Gly; Tyr, biotin-Z-Z-Gly-Gly-Gly-X-X-X-X-X-Tyr-X-X-X-X-X-Gly-Gly, where pTyr is phosphotyrosine, Z indicates aminohexanoic acid and X denotes all amino acids except cysteine (Tufts University Core Facility). Streptavidin beads (Amersham Biosciences) were incubated with a fivefold molar excess of each biotinylated library in TBST (50 mM Tris (pH 7.5), 150 mM NaCl, 0.1% Tween) for 1 h at 4 °C. Peptide-conjugated beads were packed onto disposable 1 ml chromatography columns (Bio-Rad Laboratories) (250 µl beads per column) and were rapidly washed five times with TBST.

SILAC cell culture method. As described previously[11], HeLa cells were grown in DMEM media that lacked arginine and lysine (Gibco) and dialysed FBS. The media was supplemented with heavy $^{13}C_6$-L-arginine and $^{13}C_6$-L-lysine (Cambridge Isotope Laboratories) or with $^{12}C_6$-L-arginine and $^{12}C_6$-L-lysine (Sigma). Cells were passaged five times in 'heavy' or 'light' SILAC media to ensure complete labelling.

Cell lysis and immunoblotting. Mammalian cells were lysed in buffer containing 50 mM Tris pH 7.5, 1 mM EDTA, 150 mM NaCl, 1% Nonidet P-40, 1 mM dithiothreitol, 1 mM sodium orthovanadate, and 4 µg ml^{-1} of the protease inhibitors aprotinin, leupeptin and pepstatin. Western blot analysis was carried out according to standard protocols. The following antibodies were used: Flag (Sigma), pyruvate kinase (Abcam), GAPDH (Abcam) and pan-p85 (Upstate).

Screen for pTyr-binding proteins. Five milligrams of the SILAC lysates were flowed over the peptide library columns. The 'heavy' lysate was flowed over the phosphotyrosine column, and the 'light' lysate was flowed over the tyrosine column. Lysate that had flowed through the column was re-passed over the column two times. Columns were then rapidly washed five times with TBST, and bound proteins were eluted with 250 µl 20 mM sodium phenylphosphate, pH 7.8. Entire screen protocol was conducted at 4 °C. Eluates from the phosphotyrosine and tyrosine columns were combined, the volume was condensed using a speed vacuum, and the entire SILAC sample was run on one lane of an SDS–PAGE gel.

SILAC data acquisition. The entire SDS–PAGE lane containing the SILAC labelled proteins was cut into ten pieces and each gel piece was digested with trypsin at pH 8.3 at 37 °C overnight. The peptide mixtures were then extracted from the gel pieces with 40% acetonitrile/2% formic acid and separately injected onto a reversed-phase, self-packed C_{18} microcapillary column (75-µm internal diameter × 10 cm length; New Objective Inc.). Liquid chromatography tandem mass spectrometry (LC-MS/MS) was performed using a QSTAR Pulsar I quadrupole-TOF (qTOF) mass spectrometer (Applied Biosystems/MDS Sciex) operated in positive-ion data-dependent mode with one MS survey scan followed by three MS/MS scans using a 2-min exclusion window. The nanoflow LC was operated at a flow rate of 275 nl min^{-1} using a gradient of 5% B to 38% B over 60 min followed by a wash at 95% B and 1% B column re-equilibration. The buffers consisted of 0.1% acetic acid/0.9% acetonitrile/99% water (A buffer) and 0.1% acetic acid/0.9% water/99% acetonitrile (B buffer).

Determination of SILAC ratios. Proteins were identified and SILAC ratios were determined using the Paragon algorithm in ProteinPilot software, commercially available from Applied Biosystems. The raw .wiff files were searched for both protein identification from the MS/MS scans and quantitative heavy:light ratios from the MS scan against the reversed SwissProt protein database with a 95% confidence interval. The false positive rate was determined to be less than 3%. The SILAC ratio for each protein identified was plotted by protein number versus the average heavy:light ratio for each peptide identified per protein. SILAC ratios greater than 3:1 were considered significant phosphotyrosine binding proteins.

Protein identification from silver-stained bands. Silver-stained SDS–PAGE gel pieces were excised, digested and peptides extracted as described above. The peptide mixtures were then analysed by positive-ion-data-dependent microcapillary LC-MS/MS using a LTQ 2D linear ion trap mass spectrometer (Thermo Fisher Scientific). One MS scan was followed by eight MS/MS scans. The LC conditions were the same as the SILAC experiment above except the gradient was shortened to 30 min. Proteins were identified by searching the reversed NCBI non-redundant protein database using the Sequest algorithm in Proteomics Browser Software (Thermo Fisher Scientific). The results were filtered using Xcorr cutoffs of 2.0 for 1+ ions, 2.0 for 2+ ions and 2.75 for 3+ ions as well as Sf scores of 0.4 (the Sf score is the final score for protein identification by the Proteomics Browser software based on a combination of the preliminary score, the cross-correlation and the differential between the scores for the highest scoring protein and second highest scoring protein) for all charge states. At least two peptides per protein were necessary for identification. The false positive rate was determined to be less than 2%.

Recombinant pyruvate kinase production. Human PKM2 was cloned into pET28a vector (Novagen) at NdeI and BamHI sites and expressed as an N-terminal His_6 tag fusion protein. The protein was expressed and purified with standard protocol. Briefly, pET28a-PKM2 was transformed into BL21(DE3)pLysS cells and grown to an absorbance of 0.8 at 600 nm, then induced with 0.5 mM IPTG for 7 h at room temperature. Cells were lysed by lysozyme in lysis buffer 50 mM Tris pH 8.0, 10 mM $MgCl_2$, 200 mM NaCl, 100 mM KCl, 20% glycerol, 10 mM imidazole, 1 mM PMSF; and cell lysate was cleared by centrifugation. PKM2 was purified by batch binding to Ni-NTA resin (Qiagen). The resin was then washed with lysis buffer containing 30 mM imidazole for 200 column volumes, and His_6-tag-PKM2 was eluted with 250 mM imidazole. The protein was dialysed overnight at 4 °C to remove the imidazole.

PKM2 crystal structures. His_6-tag-PKM2 was cleaved by thrombin overnight at 4 °C during dialysis (protein:dialysis buffer, 1:400). The protein was then concentrated and further purified on a Superdex 200 column (GE Healthcare Life Sciences) with buffer 25 mM Tris pH 8.0, 0.1 M KCl, 5 mM $MgCl_2$, 10% glycerol. The clean protein was pooled and concentrated to 80 mg ml^{-1} with addition of oxalate (final concentration 2 mM). Crystals were obtained from either hanging-drop or sitting-drop set-ups from a wide range of conditions with PEG3350 as the main precipitant (12–15.5% PEG3350, 100 mM Tris pH 7.2–7.5, 10% PEG400). Both *apo* crystals and FBP-bound crystals can form in the same drop with different crystal shapes. Crystals were snap frozen in liquid nitrogen after a quick dip in cryo-protectant composed of the mother liquid with 20% PEG400. Both the *apo* and FBP-bound data sets were collected at APS, NE-CAT. The initial phases were obtained using MOLREP and human PKM2 tetramer (Protein Data bank 1T5A) as the search model, the refinement was carried out with CNS and O.

Peptide library screening. A phosphotyrosine-oriented degenerate peptide library containing the sequence Gly-Gly-Gly-X-X-X-X-X-pTyr-X-X-X-X-X-Gly-Gly was synthesized (Tufts University Core Facility). Peptide library screening was performed using 100 µl nickel beads (Qiagen) containing saturating amounts of 6×His–PKM2 or 6×His–PKM1 (~1–1.5 mg) as described previously. Beads were packed in a 1-ml column and incubated with 1 mg of the peptide library mixture for 5 min at room temperature in M2 buffer (50 mM sodium bicarbonate pH 7.5, 5 mM $MgCl_2$, 150 mM NaCl, 30 mM imidazole). Unbound peptides were removed from the column by two rapid washes in the M2 buffer with 0.5% Nonidet P-40 followed by one wash with M2 buffer. Bound peptides were eluted with 500 µM FBP, lyophilized, resuspended in H_2O, and sequenced by automated Edman degradation on a Procise protein microsequencer. Selectivity values for each amino acid were determined by comparing the relative abundance of each amino acid at a particular sequencing cycle in the recovered peptides that bound to 6×His–PKM2 to that of each amino acid at the same position in the recovered peptides that bound to 6×His–PKM1.

^{14}C-FBP dialysis experiments. Freshly generated recombinant PKM1 or PKM2 protein was diluted to a concentration of 1 µM in 50 mM Tris (pH 7.5), 100 mM KCl, 5 mM $MgCl_2$, 5% glycerol. ^{14}C-FBP (MP Biomedicals) was used at 25× when added to PKM1, PKM2 or the diffusion control corresponding to a final concentration of ~10 µM ^{14}C-FBP. The PKM1, PKM2 and no-protein control were incubated with ^{14}C-FBP for 30 min at room temperature and then dialysed against >2 l of buffer using 10,000 MWCO dialysis cassettes (Peirce) for at least 7 h. After dialysis, samples were recovered and the amount of ^{14}C-FBP retained in each dialysis cassette was determined by scintillation counting. For FBP release experiments, fresh PKM2 protein was incubated with ^{14}C-FBP and dialysed as described above and the resulting sample divided into two samples. These samples were incubated with either 1 mM P-M2tide or 1 mM NP-M2tide for 30 min at room temperature, and each sample re-dialysed against >2 l of buffer using 10,000 MWCO dialysis cassettes for a minimum 7 h. Samples were recovered and the amount of ^{14}C-FBP retained was determined by scintillation counting.

Association of ^{3}H-glucose metabolites with PKM2 *in vivo*. A549 cells stably expressing Flag-tagged mouse PKM2 were washed three times with serum-free media, and incubated overnight in media with serum and 5 mM glucose spiked with ~50 nM ^{3}H-glucose. Cells were either stimulated with pervanadate for 15 min or not stimulated and lysed in NP-40 lysis buffer. Flag–PKM2 in the lysates was immunoprecipitated using Flag beads (Sigma). After a 3-h incubation period at 4 °C, beads were washed three times in lysis buffer, and ^{3}H amounts retained on PKM2 were determined by scintillation counting.

Measurement of pyruvate kinase activity. Pyruvate kinase activity was measured according to published methods by a continuous assay coupled to lactate dehydrogenase (LDH). The change in absorbance at 340 nm owing to oxidation of NADH was measured using a Victor3 1420 Multilabel Counter spectrophotometer (PerkinElmer, Inc.). Kinetic assays for activity determinations contained recombinant pyruvate kinase (20–100 ng) or cell lysate (1–2 µg), Tris

pH 7.5 (50 mM), KCl (100 mM), $MgCl_2$ (5 mM), ADP (0.6 mM), PEP (0.5 mM), NADH (180 μM), FBP (10 μM) and LDH (8 units).

Rescue constructs and retroviral production. Flag-tagged mouse PKM1, PKM2, PKM2 KE and human PKL were cloned into the retroviral vector pLHCX (Clontech) and were co-transfected into 293T cells along with an expression vector with an Ampho cassette. Retrovirus was harvested 36 h after transfection, and 5 μg ml^{-1} polybrene was added. Subconfluent H1299 and A549 cells were infected with harvested retrovirus and were selected in 350 μg ml^{-1} hygromycin for 2 weeks.

shRNA constructs and lentiviral production. shRNA constructs were provided by W. Hahn (RNAi consortium) in lentiviral cassettes. A shRNA with high pyruvate kinase knockdown efficiency was used (kd) (5′-CCGGGCTGTGGC-TCTAGACACTAAACTCGAGTTTAGTGTCTAGAGCCACAGCTTTTTG-3′), and a shRNA with no effect on pyruvate kinase levels was used as a control (cl) (5′-CCGGGAGGCTTCTTATAAGTGTTTACTCGAGTAAACACTTATAAGA-AGCCTCTTTTTG-3′). Lentivirus was made using a three-plasmid packaging system as described previously[18].

Measurement of glucose metabolism. Cellular glucose metabolism rates were measured by following the conversion of 5-^{3}H-glucose to ^3H_2O as described previously[4]. The assay was performed with cells attached to tissue culture plates. Briefly, the cells were washed once in PBS, before incubation in Krebs buffer without glucose for 30 min at 37 °C. The Krebs buffer was then replaced with Krebs buffer containing 10 mM glucose spiked with 10 μCi of 5-^{3}H-glucose. After 1 h, triplicate samples of media were transferred to PCR tubes containing 0.2 N HCl and the amount of ^3H_2O generated was determined by diffusion as described previously.

Cell proliferation analysis. 5×10^4 cells were seeded in triplicate in 6-well plates, and accurate cell counts were obtained every 24 h using a Coulter particle analyser for a 3–5-day period. Time zero was taken 16 h after seeding.

Oxygen consumption and lactate production. Oxygen consumption and lactate production were measured as described previously[16].

Measurement of ^{14}C-containing lipids. ^{14}C-containing lipids were measured as described previously[17]. Briefly, 4 μCi ml^{-1} of D-[6-^{14}C]-glucose was spiked into complete media and added to cells for 5 min before pervanadate stimulation. Cells were then stimulated with pervanadate for 10 min in the presence of labelled glucose, washed three time with PBS, and lipids extracted by the addition of hexane:isopropanol (3:2 v/v). Two serial hexane:isopropanol extracts were combined for each sample, dried under N_2, and resuspended in chloroform for scintillation counting. Cell numbers obtained by coulter counting of equally plated samples were used for normalization.

18. Root, D. E., Hacohen, N., Hahn, W. C., Lander, E. S. & Sabatini, D. M. Genome-scale loss-of-function screening with a lentiviral RNAi library. *Nature Methods* **3,** 715–719 (2006).